CALCULATION OF TRANSMISSION FUNCTIONS IN THE NEAR INFRARED REGION USING SERIES OF EXPONENTS

L.I. Nesmelova, O.B. Rodimova, and S.D. Tvorogov

Institute of Atmospheric Optics,
Siberian Branch of the Russian Academy of Sciences, Tomsk
Received July 21, 1997

Rigorous mathematical expressions for expanding the transmission functions into the series of exponents derived by the authors earlier are applied in the present paper to calculation of the water vapor transmission functions, which are necessary to evaluate the fraction of solar radiation going through the Earth's atmosphere in the near infrared region of spectrum (2800–14200 cm^{-1}). The results are compared with the data obtained using other methods.

1. In studies of the climate changes in the context of climate models the major part of calculation efforts falls on the description of absorption by atmospheric gases. To reduce the volume of calculations different approximations of the transmission functions by a series of exponents are widely applied. The mathematical problem originates from the fact that the transmission function

$$P(x) = \frac{1}{\Delta\omega} \int_{\omega_1}^{\omega_2} e^{-\varkappa(\omega)x}\, d\omega, \qquad (1)$$

(where $\varkappa(\omega)$ is the absorption coefficient at the frequency ω, x is the optical density, $\Delta\omega = |\omega_1 - \omega_2|$) should be represented as a series

$$P(x) = \sum_k c_k\, e^{-\lambda_k x} \qquad (2)$$

(c_k and λ_k are the expansion coefficients) with a minimum number of terms which is still compatible with the required calculation accuracy. The problems associated with the transition from Eq. (1) to Eq. (2) were studied in a number of papers, see, for example, Refs. 1, 2, and references therein.

Different ways of calculation of c_k and λ_k can be divided by convention into two groups using the next representations of the transmission function followed by the transition to the formulas of integration of the type of Eq. (2)

$$P(x) = \frac{1}{\Delta\omega} \int_{\omega_1}^{\omega_2} e^{-\varkappa(\omega)x}\, d\omega = \int_0^{\infty} f(s)\, e^{-ks}\, ds = \sum_\nu b_\nu e^{-xs_\nu} = \qquad (3a)$$

$$= \int_0^1 e^{-s(g)x}\, dg = \sum_\nu a_\nu\, e^{-xs(g_\nu)}. \qquad (3b)$$

In the case (3a) (see, for example, Refs. 1 and 2) the function $f(s)$ is calculated as the Laplace transform of $P(x)$ and therefore it depends on the thermodynamical parameters of the medium. Consequently, the quantities b_ν include this dependence as well. In other words, the search for optimal values of b_ν requires the calculation of polynomials orthogonal in the interval $[0, \infty)$ with the weight $f(s)$, that is too a cumbersome task that is never performed. This leads, in particular, to complexities in calculation of the integrals over inhomogeneous paths resulting in assumptions like the hypothesis on the correlated spectra for different thermodynamical conditions. Modifications of the method such as separation of the spectral lines of the absorbing gas into the groups as though they belong to some hypothetical gases,[3] the isolation of the multipliers dependent on thermodynamical characteristics from the absorption coefficients,[4] subdivision of the absorption into that the line center and in the line wing[5] attempt to overcome these difficulties. It is hard to tell whether they can be adequately resolved in this way, especially if taking into account the fact that in derivation of Eq. (3a) the mathematical actions are usually assumed, that are not rigorously substantiated (see the corresponding analysis in Refs. 6 and 7).

The approach developed by the authors[6–9] realizes the program (3b), which has some advantages as compared to (3a). Thus, rigorous expression for the function $g(s)$ was derived, so that the application of conventional formulas of integration (for example, that by Gauss or Chebyshev) results in coefficients a_ν in Eq. (3b), which are independent of thermodynamical conditions and, in addition, are optimal being associated with polynomials orthogonal in the interval $[0, 1]$. This circumstance removes the problems in the integration over inhomogeneous paths and allows one to apply this technique to evaluation of integrals including the source function.

0235-6880/97/12 923-05 $02.00

The expansion procedures using *a priori* values of the coefficients b_ν (Refs. 10, 11) are to a large extent efficient and give a solution to the problems associated with inhomogeneous paths and actually are closely related to the method developed in Refs. 6–9.

In this study, the H_2O transmission functions in the near infrared are calculated using their expansion into a series of exponents, whose coefficients according to the method[6–9] are independent of thermodynamical parameters. The comparison of the results of the present calculation with those obtained using other modifications of the expansion of the transmission functions into the series of exponents illustrates the advantages of the method developed here.

2. The line-by-line calculations of the absorption coefficients required for the construction of the $g(s)$ function by Eq. (3b) were performed by making use of the spectroscopic data base[12] with the step 0.01 cm^{-1} and with the Lorentzian line shape prolonged up to 20–25 cm^{-1} from the line center. The function $g(s)$ corresponding to the absorption coefficient at a given temperature and pressure in a given spectral interval was calculated by the formula

$$g(s) = \frac{1}{\Delta\omega} \int\limits_{\varkappa(\omega) \le s,\ \omega \in [\omega_1, \omega_2]} d\omega, \qquad (4)$$

obtained from Eq. (1) without any approximations.[6] The function $s(g)$ in the integral (3b) was found as an inverse function of $s(g)$ and the integral (3b) was represented as a sum of exponents using some variants of the Gauss and Chebyshev formulas of integration, namely, with 5, 6, 7 and 6, 7, 9 nodes, respectively. In so doing, as was mentioned above, the weights a_ν were standard for the formulas of integration, i.e. they were independent of temperature, pressure and optical density, whereas $s(g_\nu)$ were equal to the values of $s(g)$ at the points corresponding to the standard nodes of the formulas of integration. Furthermore, the transmission functions $P(x)$ at arbitrary optical densities were calculated according to Eq. (3b), i.e. the special optimization of the expansion coefficients for a wide interval of values of optical densities was not performed.

3. The general view of the H_2O spectrum in the near infrared region is shown in Fig. 1, where the line intensities are presented summed over the intervals of 10 cm^{-1}. Transmission functions and the expansion coefficients in the corresponding series of exponents were calculated for wide spectral intervals involving the H_2O absorption bands 0.72, 0.82, 0.94, 1.14, 1.38, 1.87, 2.7, and 3.2 μm. The integral transmission functions for some bands are shown in Fig. 2. The results obtained are presented in the figure for the minimum number of terms in the series, which is equal to 5. They well agree with the line-by-line calculations and with the results[10] obtained using direct fitting of the transmission functions at different optical densities by sums of exponents with prescribed weights. The relative errors of the calculations are illustrated in Fig. 3 by the example of the 1.38 μm band.

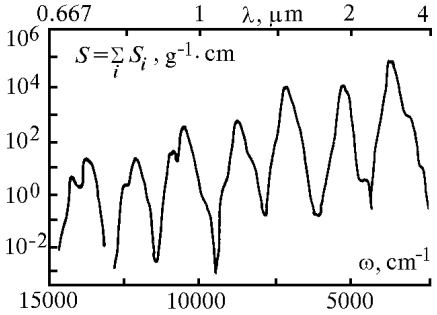

FIG. 1. Sums of intensities of the H_2O *spectral lines within the intervals of* 10 cm^{-1} *in the visible and near infrared.*

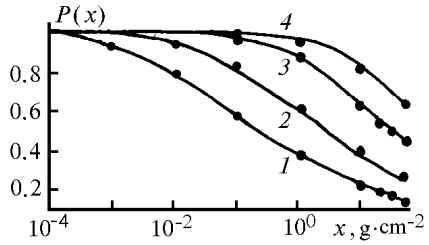

FIG. 2. Integral transmission functions for some water vapor bands in the near infrared region. Curves are calculated by the line-by-line method. Calculations[10] coincide with the curves at the scale of the figure and therefore are not shown here. The results of our calculations are marked by circles. T = 260 K, P = 500 mb. *Curves 1, 2, 3, 4 refer to the bands* 2.7, 1.38, 0.94, and 0.72 μm, *respectively.*

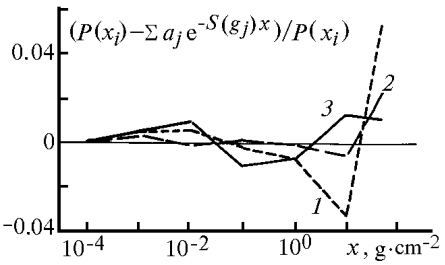

FIG. 3. Relative errors of the approximation of the transmission function calculated by the line-by-line method for the 1.38 μm *band by the series of exponent as a function of optical density. Curves 1, 2, 3 are obtained using Gauss formulas of integration with 5 and 7 nodes and by Chebyshev formulas of integration with 7 nodes, respectively.*

The results of cell measurements of spectral and integral water vapor transmission functions in the near infrared can be found in Ref. 13. The transmission functions calculated in the present paper are shown in Fig. 4 in comparison with the experimental data[13] and with that calculated in Ref. 10. The values obtained

from the empirical formulas by Moskalenko[14] are also shown in the figure. Note that use of empirical formulas in calculations of the transmission functions yields, on the whole, satisfactory results. As an example, Figure 5 shows the absorption spectrum in the 1.14 μm band, the experimental one,[13] calculated in the present paper, and that calculated with formulas.[14]

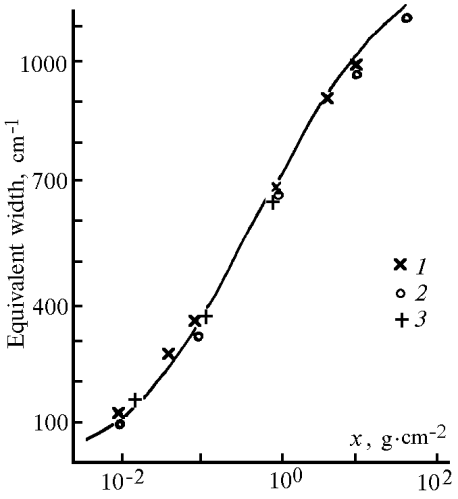

FIG. 4. Equivalent widths of the water vapor bands in the near infrared vs optical density, T = 296 K, P = 1 atm. Curve presents the experimental data,[13] 1, 2, 3 refer to calculation from Ref. 10, present calculation, and the calculation by empirical formulas.[14]

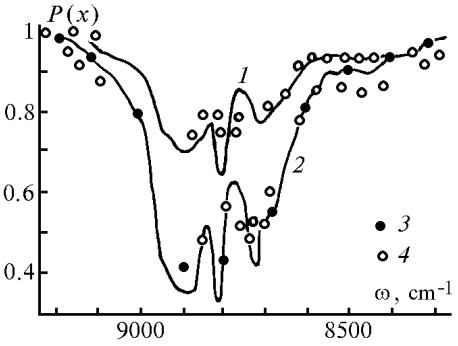

FIG. 5. Water vapor absorption spectrum within the 1.14 μm band. Curves describe experimental data[13] at P = 0.13 atm, x = 0.862 g·cm^{-2} (1) and at P = 1 atm, x = 0.853 g·cm^{-2} (2); the present calculation (3) and the results of calculation by empirical formulas[14] (4) are also shown in the figure.

In common practice, to diminish the volume of calculations the transmittance is calculated rigorously at some intermediate atmospheric conditions and then the temperature and pressure dependence is taken into account in an approximate way. Thus, in Refs. 10, and 11 a one-parameter scaling approximation is used for this purpose

$$\exp(-\varkappa_\nu(P, T)\, x) \cong \exp(-\varkappa_\nu(P_{ref}, T_{ref}\, X));$$

$$X = f(P, T)\, x = \frac{P}{P_{ref}}\, x \qquad (5)$$

with P_{ref} =500 mb, T_{ref} = 260 K. The extent to which this approximation is applicable is shown in Fig. 6. The calculation with this approximation well agrees with the line-by-line calculation at standard temperature and pressure and slightly differs from it at low temperatures and pressures. The calculation using the series of exponents coincides with the line-by-line calculations within the scale of the figure.

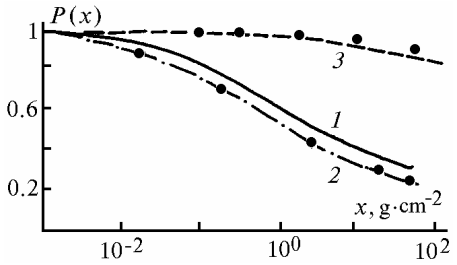

FIG. 6. Transmission functions for the 1.38 μm band. Curves present the line-by-line calculation at T=260 K, p=0.5 atm (1), T = 292 K, p = 0.9934 atm (2), T = 220 K, p = 10^{-4} atm (3); circles denote the calculation with the use of approximation (1).

The detailed calculations of the transmission functions based on the technique of their approximation by the series of exponents similar to that in Ref. 10 in the spectral region 1.125–1.135 μm were performed in Ref. 11 for the atmospheric model from Ref. 15. for the midlatitude summer. The model characteristics are listed in Table I. In Figure 7 the transmission function behavior is shown for three atmospheric layers as a function of the H_2O optical density (the curves present line-by-line calculation and the calculation[11] with the improved variant of the exponential fitting, points are the results of this paper).

TABLE I. Characteristics of the climate model.

Number of a layer	Top of layer, km	Bottom of layer, km	T, K	p, atm	x, g/cm^2
1	90.0	10.0	220.0	0.0003	$6.400\cdot10^{-5}$
2	10.0	9.5	238.0	0.2890	$4.000\cdot10^{-3}$
3	9.5	7.0	245.0	0.3558	$4.800\cdot10^{-2}$
4	7.0	5.0	261.0	0.4794	$1.217\cdot10^{-1}$
5	5.0	3.0	270.0	0.6190	$3.633\cdot10^{-1}$
6	3.0	2.0	282.0	0.7447	$4.412\cdot10^{-1}$
7	2.0	1.0	287.5	0.8394	$7.407\cdot10^{-1}$
8	1.0	0.0	292.0	0.9434	$1.141\cdot10^{0}$

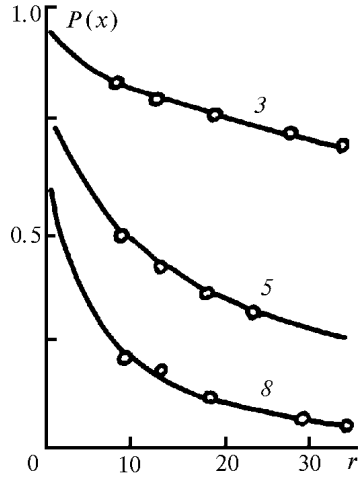

FIG. 7. Transmission functions for separate atmospheric layers in the spectral region 1125–1135 cm^{-1}. *Curves present the line-by-line calculation and the calculation[11] with the improved variant of the exponential fitting, the circles show our results, the numbers at curves are the numbers of layers.*

Figure 8 illustrates the calculations for inhomogeneous paths in the same spectral region. The curves characterize the absorption from the upper boundary of the atmosphere up to a certain layer, other notations are the same as in Fig. 7. Table II lists an example of the transmission calculation for an inhomogeneous path

$$P(l) = \sum_{\nu} a_\nu \exp\left[-\left(\sum_j s(g_\nu, l_j)\,\Delta l_j\right) m_r\right]$$

from the upper boundary of the atmosphere up to the layer l_j, with the value of the optical density chosen as in Ref. 11, i.e. $m_r = x(r/4)$, $r = 1, \ldots, 35$.

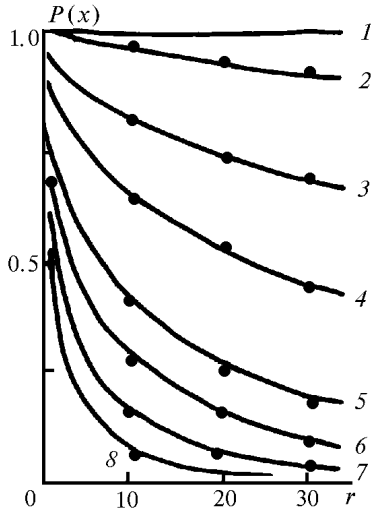

FIG. 8. Transmission functions showing the transmittance from the upper boundary of the atmosphere up to a certain layer, notations are the same as in Fig. 7.

TABLE II. Example of calculation of transmission for the inhomogeneous path, $n = 5$, $r = 10$.

	ν					
	1	2	3	4	5	
	a_ν					
	0.1185	0.2393	0.2844	0.2392	0.1185	
Number of a layer	$a_\nu \exp\left[-\left(\sum_j s(g_\nu, l_j)\,\Delta l_j\right) m_r\right]$					$P(l_1 \to l_j)$
1	0.1185	0.2393	0.2844	0.2393	0.1185	1.0
2	0.11845	0.2389	0.2834	0.2346	0.09453	0.970
3	0.1178	0.2340	0.2696	0.1780	0.0050	0.804
4	0.1157	0.2193	0.2311	0.0780	0.00001	0.415
5	0.1083	0.1737	0.1332	0.001	0.00001	0.288
6	0.09843	0.1262	0.0633	0.00001	0	0.169
7	0.0822	0.07029	0.0165	0	0	0.078
8	0.06071	0.02642	0.0017	0	0	0.034

Note in conclusion that the method of expansion of the transmission functions into the series of exponents based on the rigorous mathematical expressions for their coefficients[6–9] provides sufficient accuracy of calculation even at the absence of special procedures improving the fitting and allows one to generalize this technique to the case of more complicated integrals incorporating the transmission function while keeping mathematical rigor and simplicity of numerical calculations. Thus, the calculation for inhomogeneous paths reduces just to a few summations.

By this means the proposed method of calculations of the transmission functions is well suited for solving the climate study problems.

ACKNOWLEDGMENT

The study was supported by Russian Foundation for Basic Research, grant No. 97–05–65985.

REFERENCES

1. R. Goody, R. West, L. Chen, and D. Grisp, J. Quant. Spectrosc. Radiat. Transfer **42**, 539 (1989).
2. A.A. Lacis and V. Oinas, J. Geophys. Res. **96D**, 9027 (1991).
3. Ph. Riviere, A. Soufani, and J. Taine, J. Quant. Spectrosc. Radiat. Transfer **48**, 187 (1992).
4. V.D. q hou and A. Arking, J. Atmos. Sci. **38**, 798 (1981).
5. H.-D. Hollweg, J. Geophys. Res. **98D**, 2747 (1993).
6. S.D. Tvorogov, Atmos. Oceanic Opt. **7**, No. 3, 165–171 (1994).
7. S.D. Tvorogov, Atmos. Oceanic Opt. **10**, Nos. 4–5, 403–412 (1997).
8. S.D. Tvorogov, L.I. Nesmelova, and O.B. Rodimova, Atmos. Oceanic Opt. **9**, No. 3, 239–242 (1996).
9. L.I. Nesmelova and S.D. Tvorogov, Atmos. Oceanic Opt. **9**, No. 8, 727–729 (1996).

10. S. Asano and A. Uchiyama, J. Quant. Spectrosc. Radiat. Transfer **38**, 147 (1987).
11. W. Armbruster and J. Fischer, Appl. Opt. **35**, 1931 (1996).
12. L.S. Rothman, R.R. Gamache, R.H. Tipping, C.P. Rinsland, M.A.H. Smith, D.C. Benner, V.M. Deori, J.-M. Flaud, C. Camy-Peyret, A. Perrin, A. Goldman, S.T. Massie, L.R. Brown, and R.A. Toth, J. Quant. Spectrosc. Radiat. Transfer **48**, 469 (1992).
13. T. Yamanouchi and M. Tanaka, J. Quant. Spectrosc. Radiat. Transfer **34**, 463 (1985).
14. N.I. Moskalenko, Izv. Akad. Nauk SSSR, Fiz. Atmos. Okeana **5**, 1179 (1969).
15. R.A. McClatchey, W. Fenn, J.E.A. Selby, F.E. Volz, and J.S. Garing, *Optical Properties of the Atmosphere*, AFCRL-TR-73-0096 (U.S. Air Force Cambridge Research Laboratory, Cambridge, Mass., 1973).